High-Power RF Cavity R&D for the PEP-II B Factory*

R. Rimmer, G. Lambertson,#
LBL, 1 Cyclotron Road, Berkeley, CA 94720, USA
J. Hodgson, K. Ko, C. Ng, R. Pendleton, E. Reuter, H. Schwarz, K. Skarpaas, ‡
SLAC, 2575 Sand Hill Road, Menlo Park, CA 94025, USA
F. Adams, B. Burton, M. DeJong, M. Lipsett, †
AECL Chalk River Laboratories, Chalk River, Ontario, Canada, K0J 1J0
C. Belser, M. Franks, T. McCarville,**
LLNL, Livermore, CA 94551, USA

Abstract

We describe the development of a high-power test model of the 476 MHz RF cavity for the PEP-II B Factory. This cavity is designed to demonstrate the feasibility of a high-power design with higher-order mode (HOM) damping waveguides and the fabrication technologies involved, and it can also be used to evaluate aperture or loop couplers and various RF windows. Changes to the RF design to reduce peak surface heating are discussed and results of finite-element analyses of temperature and stress are presented. Fabrication methods for the prototype and subsequent production cavities are discussed.

1. INTRODUCTION

The PEP-II B Factory is intended to be a high-luminosity asymmetric electron-positron collider, optimized for the study of CP violation [1]. To achieve the desired integrated luminosity will require reliable operation with high average currents and many bunches, see table 1. This provides many challenges in the design of the machine, including the RF system. Single-cell copper cavities were chosen, with the expectation of reliable operation at high beam current, and the design optimized to give the highest shunt impedance for the accelerating mode so that the number of cavities is reasonable.

With careful design of the vacuum chambers the RF cavities are the largest driving impedances for coupled-bunch instabilities. In this design the HOM impedances are reduced at the source, by damping the HOMs in the cavity with dedicated waveguides [2]. The residual impedance of the damped cavity HOMs will still drive coupled-bunch oscillations but these can be damped by a practical broad-band feedback system [3].

2. OPERATING PARAMETERS

When the design of the high-power cavity was started the nominal operating voltage of the HER cavities was 0.93 MV, requiring about 122 kW of power to be dissipated in the cavity walls. This, and the addition of the ports required for HOM damping, would have produced higher than usual power density

Table 1. New PEP-II RF system parameters
(including the effect of the 5% gap in the beam)

PARAMETER	HER	LER
RF frequency (MHz)	476	476
Beam current (A)	1.03	2.25
Number of bunches	1658	≥1658
Number of cavities	24	10
Number of klystrons	6	5
Shunt Impedance R_s (MΩ) [a]	3.5	3.5
Gap Voltage (MV)	0.77	0.59
Wall loss/cavity (kW)	84.9	49.7
Coupling factor without beam (β)	3.6	3.6
Unloaded Q of cavity[b]	≥30000	≥30000

[a] $R_s = V^2/2P$

[b] with ports, at 40°C

on some parts of the cavity surface. We chose to design the cavity cooling system to handle up to 150 kW total wall loss to give some safety margin and operational flexibility.

Subsequent improvements in the machine design have reduced the beam current and cavity voltages required to meet the design luminosity, see table 1. Since the publication of the conceptual design report [1], we have had the opportunity to re-optimize the RF station [4]. In this new configuration there are four more cavities in the HER but four fewer stations, with each klystron now driving four cavities. The LER stations remain as before. The increased number of cavities in the HER means that the maximum cavity dissipation is now about 85 kW, so our 150 kW design should be very conservative.

The "factory" nature of the project requires reliable operation over the life of the machine. We chose to design for the possibility of up to 10,000 full temperature cycles of the cavity, and in this light the fatigue strengths of the materials are more important than their ultimate strengths.

3. CAVITY DESIGN

3.1. RF design

The high-power test model under development has ports for an aperture coupler and a loop coupler, a PEP-style plunger tuner and several pick-up loops, etc.. The location of the HOM damping ports was chosen to attenuate all modes and most strongly the worst HOMs. Measurements on a cold test model show that the damping scheme reduces the impedance of the worst HOMs by more than three orders of magnitude [5].

Analysis of the surface power distribution in the cavity has been carried out using the boundary-integral code LOGCABIN, [6], using surface meshes constructed in ANSYS [7], (figure 1). This analysis showed that the concentration of current towards the end of the HOM damping slots gave the highest power density in the cavity. In the first high-power design the radius on the edge between the HOM waveguide and the body was 0.25 inches (6.35 mm) and the peak power density was about 170 W/cm^2, for 150 kW total cavity dissipation. Increasing this radius to 0.5 inches (12.7 mm) reduced this peak power density to less than 120 W/cm^2. The heating profiles produced by LOGCABIN were used for input to a 3D ANSYS model of the cavity for thermal analysis.

3.2. Thermal management

The 2D mesh used by LOGCABIN was the same as the inside surface mesh of the 3D ANSYS model so the heat flux could be applied directly to the 3D model.

The cooling scheme proposed uses discrete channels routed within the cavity body and ports to provide maximum cooling to the areas with the highest heat loads. However, applying maximum cooling to the rest of the body would not produce the lowest overall stresses because the warmer regions, which will try to expand, would be in conflict with the larger cooler areas. By allowing some regions close to the hot-spots to warm up slightly the peak stresses can be reduced. The temperature distribution still closely follows the heat input, as expected (figure 2), with the maximum reaching 104 °C for 150 kW total wall loss. The temperature distribution calculated in this way was used as input to the 3D stress analysis.

3.3. Stress analysis

The highest stresses in the cavity are caused by local thermal gradients between the hot inner surface and the nearest cooling channels, and by the expansion of the warm regions with respect to the rest of the cavity.

The thermal management scheme reduces the differential expansion stresses and lowers the peak Von Mises stress by around 30 %, to about 10,000 psi (69 MPa), see figure 3. The small increase in average temperature lowers the cavity Q by less than 1%, which is acceptable.

Stresses in the body due to gravity and atmospheric pressure are small compared to the thermal stresses and stresses in the port subassemblies should be minimal since they will become annealed during brazing, but stresses from weld shrinkage during assembly may be significant. If the material of the port inserts, where the peak thermal stresses are induced, is fully annealed during manufacture then during shrinkage of the weld the soft material will yield preferentially, although the strain will be limited by the stiffness of the body. In this case the outcome can be no more than about 10,000 psi (69 MPa) tensile static stress in addition to the peak cyclic thermal stress which is also about 10,000 psi but is compressive. Under these conditions the fatigue strength for fully annealed OFHC copper at 10,000 cycles is about 16,000 psi (110 MPa), compared to about 19,000 psi (131 MPa) with zero mean stress [8], so the design is still
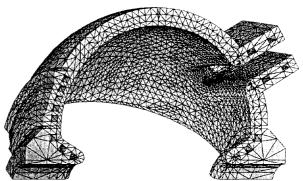

Figure 1. Finite-element mesh for ANSYS thermal and stress models, the surface of which is used by the LOGCABIN code to solve for RF current distribution.
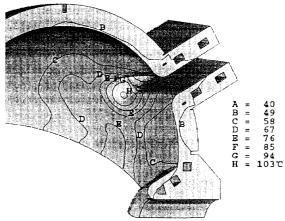

Figure 2. Temperature distribution of a section of the cavity calculated by ANSYS for 150 kW total wall loss. Note the peak is towards the end of the HOM damping aperture, where the current is concentrated.
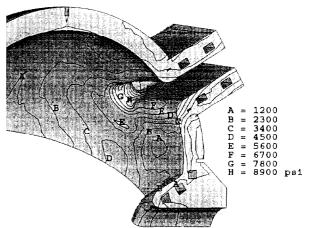

Figure 3. Von Mises stress distribution around the HOM port calculated for 150 kW wall dissipation. Peak thermal stress is at the end of the HOM damping aperture and is compressive.

conservative even with possible built-in stresses and 150 kW wall loss. Operating the cavity at 85 kW provides a further large safety factor.

4. MECHANICAL DESIGN AND FABRICATION

One goal of this high-power cavity is to demonstrate the viability of a possible fabrication method. The raw materials used are class 2 [9] OFHC copper for the body and ports, plus some non-magnetic stainless steel for the flanges, etc. The body is made by deep drawing two bowls from plates, using a hydraulic press, which are joined together by electron-beam welding around the equator. One bowl has a small hole in the center for a nose-cone assembly, the other has a larger hole which allows easy access to the inside of the cavity and which will eventually be filled by a "lid" containing the other nose-cone (figure 4). Once the two bowls are joined the cooling passages will be cut into the body using a 5-axis milling machine. These will then be filled with wax, activated, and covered by electroforming. Index marks on the inside of the bowls will provide a way to find the channels again later.

Once a sufficient thickness of copper has been deposited on the outside of the cavity the body will be cleaned up, the inlet and outlet points of each channel will be drilled out and the wax removed. The holes for the various ports will then be roughed out, the openings for the HOM ports will be finish-machined and the HOM port subassemblies will be electron-beam welded into place. After this, each of the equatorial openings in turn will have its port electron-beam welded in place. The port subassemblies, nosecones and lid have integral cooling passages and will be pre-assembled separately, by brazing. Once all of the port assemblies have been joined to the body, the inside surface and the lid opening will be finish machined. At this stage the lid and nosecones will be clamped in place and trimmed to set the frequency. The lid and nose-cones will be fixed in place with full-penetration electron-beam welds, which will be smoothed over inside by a cosmetic weld, made through the nose-cone apertures. The frequency shift due to final weld shrinkage will be measured and will be compensated for in the production versions of the cavity. These will be pre-assembled on rafts before installation in the tunnel (figure 5), and could be tested and conditioned like this.
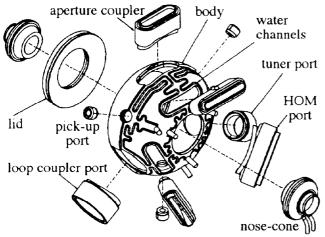

Figure 4. Assembly of high-power cavity body showing body cooling channels on one half (exposed), equatorial and HOM port inserts, nosecones and "lid" section.
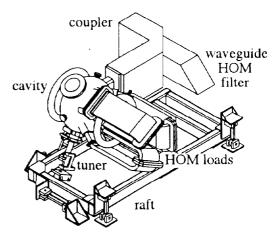

Figure 5. Conceptual layout of production cavity, coupler, tuner and HOM load assembly on raft for installation.

5. CONCLUSIONS

The R&D of the high-power cavity for PEP-II is well advanced. Minor improvements to the RF design have been made to lower the surface power density and the major engineering challenges of cooling and fabrication have been addressed. Optimization of the PEP-II RF system parameters has reduced the demands on the cavities so the design is now even more conservative. Construction of a pre-production test cavity has started, using fabrication methods which are thought to be suitable for the production cavities. The finished high-power cavity is eagerly awaited. This paper summarizes the work of a large number of people within the various groups collaborating on the PEP-II project. We are grateful to everyone who has contributed to the R&D effort.

6. REFERENCES

[1] "PEP-II, An Asymmetric B Factory", Conceptual Design Report, June 1993, LBL-PUB-5379, SLAC-418, CALT-68-1869, UCRL-ID-114055, UC-IIRPA-93-01.

[2] "RF Cavity Development for the PEP-II B Factory", R. A. Rimmer, Proc. Int. Workshop on B-Factories, BFWS92, KEK, Japan, Nov. 17-20, 1992.

[3] "Bunch-by-Bunch Longitudinal Feedback System for PEP-II", R. Claus et. al., Proc EPAC 94, June 27-July 1 1994, London.

[4] "RF System Design for the PEP-II B Factory", H. Schwarz, SLAC; R. Rimmer, LBL, for the PEP-II RF Group, Proc EPAC 94, June 27-July 1 1994, London.

[5] "Measurements of Higher Order Mode Damping in the PEP-II Low-Power Test Cavity", R. A. Rimmer and D. A. Goldberg, Proc US PAC, Washington DC, May 17-20th 1993.

[6] "Cavity RF Mode Analysis Using a Boundary-Integral Method", M.S. de Jong and F.P. Adams, Proceedings of the 1993 Particle Accelerator Conference, Washington, May 1993, pp 835-837.

[7] Swanson Analysis Systems Inc., P.O. Box 65, Houston, PA 15342

[8] "Low-temperature Mechanical Properties of Copper and Selected Copper Alloys", Richard P. Reed and Richie P. Mikesell, National Bureau of Standards Monograph 101, Issued Dec.1, 1967.

[9] "Standard Specification for Oxygen Free Copper in Wrought Forms for Electron Devices", ASTM designation F68-82.